



Recent Advances in Magnetic Fe^{x+}/TiO₂ Microfibers for Wastewater Treatment as Climate Change Mitigation

Misriyani ^{1,*}, Yang Tian ², Z. Ryan Tian ²

¹ Department of Medical Education, Faculty of Medicine, University of Alkhairaat, Palu, Indonesia

² Department of Chemistry and Biochemistry, University of Arkansas, Fayetteville, Arkansas, USA

* Corresponding author: misriyani85@gmail.com, misriyani85@unisapalu.ac.id

<https://doi.org/10.14710/jksa.27.8.403-408>



Article Info

Article history:

Received: 05th May 2024

Revised: 13th August 2024

Accepted: 26th August 2024

Online: 31st August 2024

Keywords:

Magnetic Fe^{x+}/TiO₂ Microfibers;
Degradation; Methylene Blue;
Photocatalytic

Abstract

Chemical dyeing and finishing processes used in the clothing and textile industries are among the main contributors that can increase the impact of climate change. Photocatalysis using nanosized titanium dioxide (TiO₂) has been continuously developed as a promising technology for purifying dye wastewater into simpler and environmentally friendly components. In addition, the decoration of iron cations (Fe²⁺) and (Fe³⁺) increases the reusability of the photocatalyst due to their magnetic properties, which are easy to collect for the recycling process. Magnetic Fe^{x+}/TiO₂ microfibers have been successfully prepared using a hydrothermal method using titanium dioxide in an alkaline solution. Cations were added into the solution with the different molar ratios of Ti/Fe^{x+} to produce Fe²⁺/TNW and Fe³⁺/TNW, respectively. Photocatalysis activity test using magnetic Fe^{x+}/TNW was carried out using methylene blue in a reactor equipped with an incandescent bulb lamp representing solar light. The results showed that adding the cations resulted in a new shape of palm tree leaves, like titanate microfibers. Controlling the cation's molar ratio produces the magnetic Fe^{x+}/TNW with a 50-150 μm length. SEM images of each material presented the uniformly elongated shape and aggregated on one side morphology. In addition, paramagnetic properties indicate that magnetic Fe^{x+}/TNW can be easily separated from the dispersion in less than 1 minute using an external magnet. A photocatalysis activity test of magnetic Fe^{x+}/TNW was performed by calculating the percent degradation of methylene blue with variations in irradiation time in visible light conditions. The result showed the effectiveness of photodegradation of methylene blue was significantly increased in materials with 3.3 molar ratios of both Ti/Fe²⁺ and Ti/Fe³⁺ with a percent degradation reaching 79% and 70%, respectively, in 5 hours. In conclusion, magnetic Fe^{x+}/TNW is introduced as an alternative dye wastewater treatment technology that has reusable properties and works well on sustainable energy sources of solar light.

1. Introduction

Global water scarcity is increasing. Clean water sources are starting to be abandoned because they have been contaminated by pollutant components such as heavy metals, toxic compounds, and pathogenic microbes from water pollution, dyeing, and industrial waste. As reported by UNICEF, by 2025, it is estimated that 1.8 billion people will live in water-scarce areas, affecting two-thirds of the world's population [1]. According to the first U.S. Intelligence Community Assessment on Global

Water Security, it is estimated that by 2030, humanity's annual global water demand will exceed the current sustainable water supply by 40% [2]. Wastewater from the fashion industry is one of the biggest contributors to contaminants and causes 20% of water pollution in the world [3].

Chemical dyeing and finishing processes used in the clothing and textile industries are one of the main contributors to climate change. By 2030, 102 million tonnes of clothing are expected to be consumed, with

these significant water-intensive processes contributing to 3% of global CO₂ emissions [4]. Undoubtedly, this increases greenhouse gas emissions that contribute to climate change. Without pretreatment, dyestuff waste can contaminate rivers, oceans, and surface waters and even irrigate rice fields. Countries like China, Bangladesh, Thailand, and Indonesia, which dominate the dyeing industry, face this serious issue. Human activities and environmental processes disrupt the water cycle, creating a global problem that impacts not only the life and health of organisms but also the economy, jobs, and security [5, 6, 7]. A scientific approach is needed to overcome the problem of the long-term availability of safe and healthy clean water.

Membrane filtration and adsorption techniques have recently become popular for removing effluent pollutants. However, fouling deposits on the membrane filter reduce the efficiency of the technique. The adsorption process is also suspected to produce new sludge after it is saturated to absorb contaminants. Pollutant degradation using photocatalytic reactions is a new alternative that utilizes hydrogen peroxide from photocatalyst materials induced by light. The development of new particle sizes and shapes is one factor that maximizes the various applications of nanomaterials. Titanium in microfiber form has been applied in bacterial sterilization, bone implants, controlled drug delivery, and bioscaffold applications [8, 9].

On the other hand, TiO₂ photoactivity in UV reduces applications using solar light because it represents only 5% of solar radiation. Several methods are required to increase photoactivity in visible light. Previous studies have been reported regarding the synthesis and modification of TiO₂ morphology, as well as investigations to shift the absorption activity of TiO₂ using Ag, Pt, and Mn metals, and succeeded in shifting towards longer wavelengths (redshift) [10, 11, 12, 13]. In this study, magnetic and visible-light-driven photocatalysts were successfully developed with iron metal doping to improve the reusability of the material and increase the response of TiO₂ to visible light as a representation of solar light.

2. Experimental

This study investigated the potential of iron-doped titanium dioxide (TiO₂) microfibers for degrading methylene blue. Commercially available Aeroxide P25 TiO₂ powder served as the base material, while sodium hydroxide facilitated its conversion into sodium titanate microfibers through hydrothermal treatment. Iron(III) and iron(II) chloride salts were then incorporated into these microfibers at various ratios to create magnetic Fe^{x+}/TNW. X-ray diffraction (XRD) and scanning electron microscopy (SEM) analyzed the crystal structure and morphology of the synthesized microfibers, while a UV-visible spectrophotometer played a dual role in determining their band gap energy and evaluating their effectiveness in degrading the target pollutant under visible light irradiation.

2.1. Materials

The materials used in this study were Aeroxide P25 titanium dioxide (TiO₂) powder, sodium hydroxide pellets (NaOH) (Macron Fine Chemicals), iron(III) chloride 97% (Sigma Aldrich), iron(II) chloride anhydrous 99.5% (Alfa Aesar) and methylene blue 1% (w/v) in aqueous solution.

2.2. Instrumentation

The crystallinity of iron-doped TiO₂ microfibers was measured with an X-ray diffractometer (Rigaku MiniFlex II). Scanning electron microscopy (TESCAN VEGA) and microscope (Olympus BX41) to map the image and morphology of the sample performed at 10kV. UV-Vis spectrophotometer Shimadzu UV-1280 was used to determine the band gap energy and photocatalytic activity analysis, and a mini autoclave (Parr USA) was utilized for hydrothermal synthesis.

2.3. Procedures

2.3.1. Synthesis of Fe^{x+}/TiO₂ Microfibers

First, sodium titanate microfibers were prepared using the hydrothermal method, as reported in a previous study [14]. A total of 0.125 g of TiO₂ nanoparticles was mixed with 10 M alkaline solution and stirred magnetically for 2 hours. The mixture was then subjected to ultrasonic treatment for 15 minutes until a milky white suspension formed. This suspension was transferred to a Teflon-lined autoclave and heated at 240°C for 72 hours. After cooling to room temperature, the samples were washed repeatedly with distilled water until a neutral pH was achieved, resulting in the formation of sodium titanate microfibers.

The cations of Fe²⁺ and Fe³⁺ doped TiO₂ microfibers were synthesized by mixing iron salts with sodium titanate microfibers at molar ratios of Ti/Fe^{x+} 2.5:1, 3.3:1, 4.6:1, and 10:1 to produce magnetic Ti/Fe²⁺ and Ti/Fe³⁺ microfibers respectively. The mixture was magnetically stirred for 2 hours to obtain a milky homogeneous suspension, followed by ultrasonic degassing for 15 minutes and an additional 5 minutes of stirring. The suspension was then placed in a Teflon-lined autoclave and subjected to hydrothermal treatment as described above. Finally, the sample was prepared for further characterization using XRD and SEM (Philips SEM XL30).

2.3.2. Dyes Removal

The degradation of methylene blue dye was carried out using 0.025 g of Fe^{x+}/TiO₂ in 10 mL of 5 ppm methylene blue solution. The mixture was exposed to visible light for 5 hours using an incandescent lamp as a light source. During the sampling process, small samples were taken every 30 minutes. The supernatant was then separated by centrifugation, and the absorbance was analyzed using a UV-Visible spectrophotometer.

3. Results and Discussion

3.1. SEM Analysis

The results revealed significant differences in surface morphology after iron doping, leading to the formation of magnetic Fe^{x+}/TiO₂ microfibers. These

microfibers were synthesized by stirring in a sodium hydroxide solution, followed by hydrothermal treatment. Notable differences were observed in the titanate microfibers: the undoped microfibers had wire lengths ranging from 20 to 100 μm (average 60 μm), while the iron-doped microfibers formed aggregates measuring 50 to 100 μm (average 75 μm), as shown in Figures 1a and 1b.

The alkaline hydrothermal process converts the TiO_2 nanoparticles into long and fiber-like microfibers. The presence of cations causes the fibers to become tightly packed on one side while spreading out on the other. This addition of cations in the solution resulted in a new structure resembling palm tree leaves, similar to titanate microfibers (Figure 1c). The paramagnetic properties of $\text{Fe}^{x+}/\text{TiO}_2$ microfibers allow them to be easily separated from the dispersion in less than 1 minute, turning the dark dispersion transparent with the use of an external magnet (Figure 1d). This demonstrates the excellent and easy reusability of $\text{Fe}^{x+}/\text{TiO}_2$ microfibers for removing residual materials from wastewater.

The difference in the molar ratio of Ti/Fe^{x+} caused variations in shape and length. A higher concentration of doping cations led to the formation of more aggregates and longer wire lengths. In contrast, a lower concentration of cations may prevent aggregate formation, resulting in individual microfibers with shorter wire lengths, as shown in Figure 2.

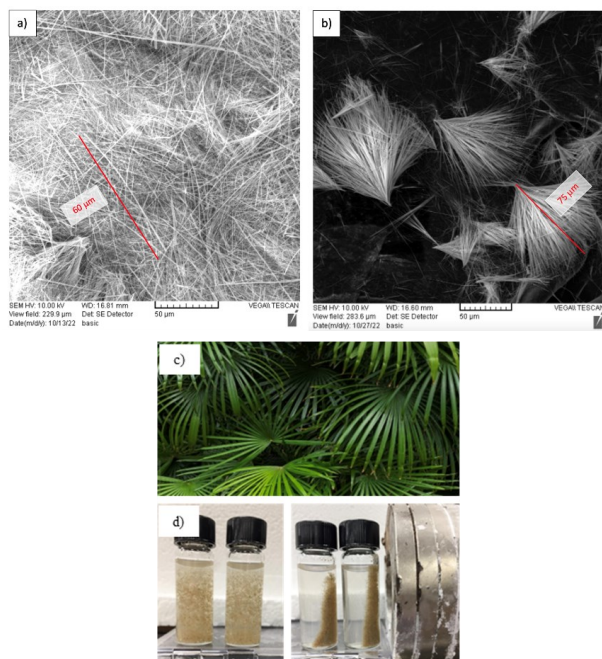


Figure 1. a–b) SEM images of titanate microfibers, c– d) cations doped titanate microfibers

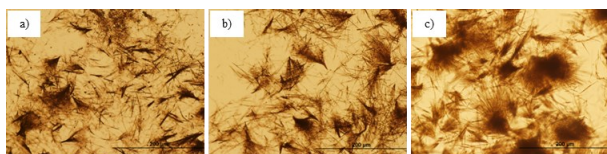


Figure 2. Microscope images of cation-doped titanate microfibers at different molar ratios of Ti/Fe^{x+} : a) 2.5, b) 3.3, and c) 4.6

3.2. XRD Analysis

The magnetic $\text{Fe}^{x+}/\text{TiO}_2$ microfibers exhibited an XRD pattern, as shown in Figure 3. This pattern includes three characteristic peaks corresponding to the typical anatase crystal structure of pure TiO_2 at $2\theta = 25^\circ, 37^\circ,$ and 38° , with specific peaks at (101), (103), and (004), according to JCPDS No. 21-1276 [15]. Fe^{2+} and Fe^{3+} doping do not significantly change the structure of pure TiO_2 . However, there is a noticeable peak shift at $2\theta = 38^\circ$ towards a higher 2θ value, indicating a change in d-spacing. According to Bragg's equation $n\lambda = 2d\sin\theta$, an increase in θ results in a decrease in d-spacing, reflecting changes in the distance between the lattice planes [13, 16].

The addition of Fe^{2+} and Fe^{3+} ions leads to a decrease in both the size and regularity of the crystal lattice. Smaller crystallite sizes result in peak broadening in the XRD pattern due to the Scherrer effect; as crystallite size decreases, the XRD peaks become broader. Iron ions slow down the growth of TiO_2 by occupying the same lattice sites as Ti^{4+} ions, causing lattice deformation due to the difference in ionic radii. Despite this, the substitution of Fe^{2+} and Fe^{3+} for Ti^{4+} ions has been successful. The integration of Fe into the TiO_2 matrix is facilitated by the similar ionic radii of Fe^{3+} (0.65 Å) and Ti^{4+} (0.68 Å) [17]. This successful substitution is further evidenced by the noticeable change in morphology, with TiO_2 microfibers resembling palm tree leaves as observed under a microscope and SEM. However, further studies are needed to fully understand the effects of ion addition on particle size distribution, structure, and phase.

3.3. Band Gap Energy Analysis

Band gap energy shift analysis was conducted using a UV-Vis spectrophotometer, with the Kubelka-Munk function used to plot the band gap energy for various iron doping ratios on TiO_2 . The analysis shows that the band gap energy decreases with increasing amounts of iron, as depicted in the band gap energy curves (Figure 4).

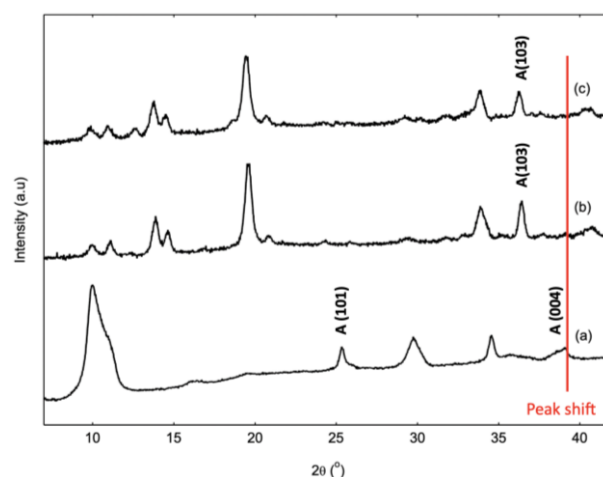


Figure 3. XRD pattern of microfibers (a) TiO_2 , (b) $\text{Fe}^{2+}/\text{TiO}_2$, and (c) $\text{Fe}^{3+}/\text{TiO}_2$

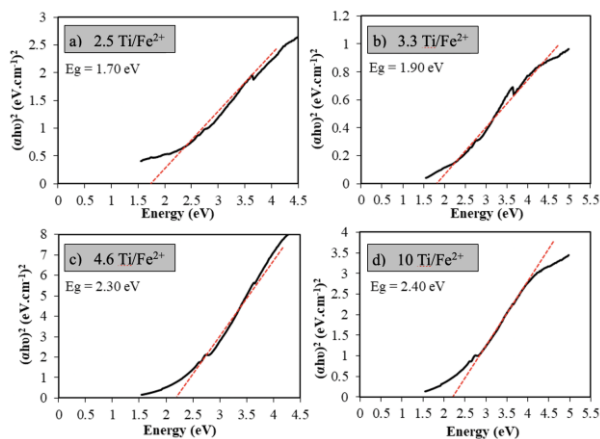


Figure 4. Kubelka-Munk reflection plots from UV-Vis spectroscopy measurements of Fe-doped TiO₂ nanoparticles at molar ratios of (a) 2.5, (b) 3.3, (c) 4.6, and (d) 10 Ti/Fe²⁺

UV-visible spectroscopy shows that doping TiO₂ with Fe²⁺ reduces the band gap energy from 2.4 eV to 1.7 eV. Increasing the amount of iron shifts the band gap energy towards longer wavelengths in the visible region. This shift is attributed to the formation of a new energy level between the conduction and valence bands of TiO₂ [18]. The new energy level facilitates electron excitation when exposed to visible light. In this study, the reduced band gap absorption in Fe-doped TiO₂ is due to charge transfer transitions between the d electrons of Fe²⁺ and the valence and conduction bands of TiO₂ [19]. Electron transitions from the valence band to the Fe dopant level or from the Fe dopant level to the conduction band effectively contribute to the red shift in absorption. The d-electron energy level of the Fe dopant can be easily excited into the conduction band of TiO₂ particles [20].

The successful incorporation of Fe²⁺ ions into TiO₂ crystals significantly influences the morphology, magnetic properties, and photoactivity of the material, enhancing its ability to degrade wastewater. The photodegradation capability of Fe^{x+}/TiO₂ microfibers, when exposed to visible light, is demonstrated using methylene blue dye as a model waste, as discussed in the following chapter.

3.4. Photocatalytic Activity of Fe^{x+}/TiO₂ Microfibers under Visible Light Exposure

Figure 5 shows the percentage degradation of methylene blue by Fe²⁺/TiO₂ and Fe³⁺/TiO₂ microfibers at different irradiation times under visible light exposure. The degradation percentage increases even within 30 minutes, reaching 39% for 10 Ti/Fe²⁺ and 47% for Ti/Fe³⁺. Fe-doping does not affect the TiO₂ crystal structure but changes its magnetic properties from diamagnetic to paramagnetic [21]. The magnetic test results in Figure 1d indicate that the Fe-doped TiO₂ material exhibits paramagnetic properties, as evidenced by its adherence to the tube wall closest to the external magnet. This behavior suggests a magnetic interaction between the intrinsic magnetic moments of the Fe ions within the material and the external magnetic field. Doping with Fe³⁺ ions enhances photocatalytic performance compared to doping with Fe²⁺ ions. The percentage degradation of methylene blue is highest for the magnetic Fe²⁺/TiO₂ and Fe³⁺/TiO₂ microfibers after 3 hours of visible light irradiation. Longer irradiation times increase the percentage degradation of methylene blue. Photocatalytic degradation occurs when TiO₂ absorbs photon energy, exciting electrons from the valence band to the conduction band and leaving holes in the valence band.

Hydroxyl radicals ($\cdot\text{OH}$) formed during this process disrupt the conjugation system of the methylene blue molecule, leading to its decomposition [13, 22]. However, prolonged irradiation can lead to further degradation of the product, potentially reducing the interaction between the photocatalyst and light, which decreases the effectiveness of methylene blue degradation. Additionally, increasing the molar ratio of cations doped into TiO₂ enhances the degradation of methylene blue, reaching an optimal value at 3.3 Ti/Fe²⁺ and Ti/Fe³⁺, with percent degradation of 79% and 70%, respectively. The presence of cations as visible-light-driven photocatalysts reduces the band gap energy of TiO₂ and shifts its absorption to the visible wavelength. However, an excess of cations can lead to the formation of clusters that cover the surface of TiO₂ and obstruct light, potentially diminishing photocatalytic efficiency.

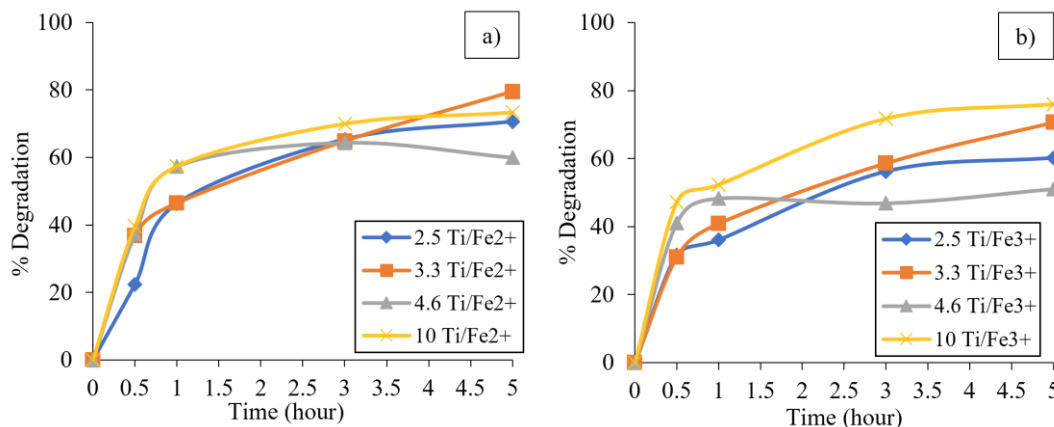


Figure 5. Photocatalytic degradation of methylene blue under visible light irradiation at different iron molar ratios and times: a) ferrous cation (Fe²⁺) and b) ferric cation (Fe³⁺)

4. Conclusion

This study successfully developed magnetic Fe²⁺/TiO₂ microfibers for the degradation of dye pollutants in wastewater to meet water quality standards. Previous research indicated that hydrothermal synthesis produced microfibers with lengths of up to 20–100 μm. In this study, the addition of cations adjusted the average fiber length to 75 μm, enhancing their effectiveness for wastewater treatment by increasing the surface area available for pollutant contact. The paramagnetic properties of the nanomaterials facilitate their reuse. By optimizing synthesis parameters and application conditions, the material's characteristics can be fine-tuned to achieve the best performance in dye removal. Ultimately, this straightforward photocatalytic degradation method using magnetic Fe²⁺/TiO₂ microfibers effectively produces large quantities of dye-free, safe water.

Acknowledgment

The authors would like to thank the Department of Chemistry and Biochemistry, Institute for Nanoscience and Engineering, University of Arkansas, and the Fulbright-AMINEF grant (Fulbright visiting scholar/Postdoctoral Program) for facilities and financial support.

References

- [1] UNICEF, Water scarcity, *Addressing the growing lack of available water to meet children's needs.*, (2022), (accessed September 23rd, 2020) <https://www.unicef.org/wash/water-scarcity>
- [2] Stewart M. Patrick, The Coming Global Water Crisis, (2012), (accessed September 23rd, 2022) <https://www.theatlantic.com/international/archive/2012/05/the-coming-global-water-crisis/256896/>
- [3] Alan Hudd, Dyeing for fashion: Why the clothes industry is causing 20% of water pollution, (2022), (accessed October 31st, 2022) <https://www.euronews.com/green/2022/02/26/dyeing-for-fashion-why-the-fashion-industry-is-causing-20-of-water-pollution>
- [4] Clean Clothes Campaign, Climate Change, (accessed August 12th, 2024) <https://cleanclothes.org/climate-change>
- [5] Tiphonie Deblonde, Carole Cossu-Leguille, Philippe Hartemann, Emerging pollutants in wastewater: A review of the literature, *International Journal of Hygiene and Environmental Health*, 214, 6, (2011), 442-448 <https://doi.org/10.1016/j.ijheh.2011.08.002>
- [6] Sana Khalid, Muhammad Shahid, Natasha, Irshad Bibi, Tania Sarwar, Ali Haidar Shah, Nabeel Khan Niazi, A Review of Environmental Contamination and Health Risk Assessment of Wastewater Use for Crop Irrigation with a Focus on Low and High-Income Countries, *International Journal of Environmental Research and Public Health*, 15, 5, (2018), 895 <https://doi.org/10.3390/ijerph15050895>
- [7] Xander Vagg, A Coming Water Crisis?, *American Security Project*, (2012), (accessed September 23rd, 2022) <https://www.americansecurityproject.org/a-coming-water-crisis/>
- [8] Wenjun Dong, Tierui Zhang, Michelle McDonald, Carmen Padilla, Joshua Epstein, Z. Ryan Tian, Biocompatible nanofiber scaffolds on metal for controlled release and cell colonization, *Nanomedicine: Nanotechnology, Biology and Medicine*, 2, 4, (2006), 248-252 <https://doi.org/10.1016/j.nano.2006.10.005>
- [9] Wenjun Dong, Tierui Zhang, Joshua Epstein, Lisa Cooney, Hong Wang, Yanbin Li, Ying-Bing Jiang, Andrew Cogbill, Vijay Varadan, Z. Ryan Tian, Multifunctional Nanowire Bioscaffolds on Titanium, *Chemistry of Materials*, 19, 18, (2007), 4454-4459 <https://doi.org/10.1021/cm070845a>
- [10] Misriyani Misriyani, Abdul Wahid Wahab, Paulina Taba, Jarnuzi Gunlazuardi, Effect of Anodizing Time and Annealing Temperature on Photoelectrochemical Properties of Anodized TiO₂ Nanotube for Corrosion Prevention Application, *Indonesian Journal of Chemistry*, 17, 2, (2017), 219-227 <https://doi.org/10.22146/ijc.24183>
- [11] E. S. Kunarti, Misriyani, Synthesis and Photoelectrochemical Activity of TiO₂ Nanotube Based Free Standing Membrane, *Asian Journal of Chemistry*, 32, 11, (2020), 2739-2742 <https://doi.org/10.14233/ajchem.2020.22764>
- [12] Misriyani, Abdul Wahid Wahab, Paulina Taba, Jarnuzi Gunlazuardi, Synthesis of TiO₂ Nanotube Decorated Ag as Photoelectrode: Application for Corrosion Prevention of Stainless Steel 304 Under Visible Light Exposure, *International Journal of Applied Chemistry*, 11, 5, (2015), 611-619
- [13] Misriyani Misriyani, Eko Sri Kunarti, Masahide Yasuda, Synthesis of Mn(II)-Loaded Ti_xSi_{1-x}O₄ Composite Acting as a Visible-Light Driven Photocatalyst, *Indonesian Journal of Chemistry*, 15, 1, (2015), 43-49
- [14] Z. Ryan Tian, *TiO₂ nanostructures, membranes and films, and methods of making same*, US8883115B2, University of Arkansas Technology Development Foundation, 2014
- [15] Dongfang Yang, *Titanium Dioxide: Material for a Sustainable Environment*, IntechOpen, Rijeka, 2018, <https://doi.org/10.5772/intechopen.70290>
- [16] Sri Hilma Siregar, Prasetya Prasetya, Norramizawati Norramizawati, Marlian Marlian, Aulia Rizki Ramadhanti, Titanium Dioxide (TiO₂) Modified Bentonite for Photodegradation in Methylene Blue Dye, *Jurnal Kimia Sains dan Aplikasi*, 26, 4, (2023), 143-150 <https://doi.org/10.14710/jksa.26.4.143-150>
- [17] M. A. Majeed Khan, Rahul Siwach, Sushil Kumar, Abdulaziz N. Alhazaa, Role of Fe doping in tuning photocatalytic and photoelectrochemical properties of TiO₂ for photodegradation of methylene blue, *Optics & Laser Technology*, 118, (2019), 170-178 <https://doi.org/10.1016/j.optlastec.2019.05.012>
- [18] Saji George, Suman Pokhrel, Zhaoxia Ji, Bryana L. Henderson, Tian Xia, Linjiang Li, Jeffrey I. Zink, André E. Nel, Lutz Mädler, Role of Fe Doping in Tuning the Band Gap of TiO₂ for the Photo-Oxidation-Induced Cytotoxicity Paradigm, *Journal of the American Chemical Society*, 133, 29, (2011), 11270-11278 <https://doi.org/10.1021/ja202836s>
- [19] Marcus Einert, Pascal Hartmann, Bernd Smarsly, Torsten Brezesinski, Quasi-homogenous photocatalysis of quantum-sized Fe-doped TiO₂ in

- optically transparent aqueous dispersions, *Scientific Reports*, 11, 1, (2021), 17687
<https://doi.org/10.1038/s41598-021-96911-6>
- [20] M. S. Shalaby, N. M. Yousif, Hadeer Gamal, Mohammed O. Alziyadi, Fe dopant controlled the ferromagnetic, structural, thermal, optical, and electrical characteristics of CdO nanoparticles, *Results in Chemistry*, 7, (2024), 101260
<https://doi.org/10.1016/j.rechem.2023.101260>
- [21] M. Yeganeh, N. Shahtahmasebi, A. Kompany, M. Karimipour, F. Razavi, N. H. S. Nasralla, L. Šiller, The magnetic characterization of Fe doped TiO₂ semiconducting oxide nanoparticles synthesized by sol-gel method, *Physica B: Condensed Matter*, 511, (2017), 89-98
<https://doi.org/10.1016/j.physb.2017.02.010>
- [22] Idrees Khan, Khalid Saeed, Ivar Zekker, Baoliang Zhang, Abdulmajeed H. Hendi, Ashfaq Ahmad, Shujaat Ahmad, Noor Zada, Hanif Ahmad, Luqman Ali Shah, Tariq Shah, Ibrahim Khan, Review on Methylene Blue: Its Properties, Uses, Toxicity and Photodegradation, *Water*, 14, 2, (2022), 242
<https://doi.org/10.3390/w14020242>